Light and heavy excitons in strained CdTe/CdZnTe quantum wells

© L.V. Kotova[1,2], D.D. Belova[1], R. Andre[3], H. Mariette[3,4], V.P. Kochereshko[1]

[1] Ioffe Institute,
194021 St. Petersburg, Russia
[2] ITMO University,
197101 St. Petersburg, Russia
[3] Institut Neel CNRS,
F-38000 Grenoble, France
[4] Japanese-French laboratory for Semiconductor Physics and Technology J-F AST,
CNRS, Universite Grenoble Alpes,
University of Tsukuba, Japan

E-mail: kotova@mail.ioffe.ru

Received April 17, 2023
Revised April 21, 2023
Accepted April 21, 2023

The spectra of photoluminescence and polarized reflection under normal and oblique incidence of light from structures with quantum wells with symmetric $Cd_{0.9}Zn_{0.1}Te/CdTe/Cd_{0.9}Zn_{0.1}Te$ and asymmetric $Cd_{0.9}Zn_{0.1}Te/CdTe/Cd_{0.4}Mg_{0.6}Te$ barriers have been studied. Due to the mechanical stresses caused by the mismatch of the crystal lattices of the wells and barriers, the energy of light holes in quantum wells was higher than in barriers, i.e., the band structure for them was of type II. However, in the reflection spectra, the lines of heavy and light excitons had comparable intensities. In structures with symmetric barriers, exciton resonances, which do not appear in the photoluminescence spectra, were found in the reflection spectra. A detailed calculation of the energy levels and reflection spectra has been carried out

Keywords: quantum well, reflection, excitons, strain.

DOI: 10.21883/SC.2023.03.56231.4803

1. Introduction

Semiconductors $A^{II}B^{VI}$, such as CdTe and ZnTe, are often used as model objects for fundamental research. Until recently, their practical application has been very limited. They were mainly used as X-ray detectors and phosphors. At the same time, they have a high structural perfection and unique optical properties. In recent years, $A^{II}B^{VI}$ compounds are increasingly being considered as materials for use in solar energy [1]. They have a high quantum yield in the spectral range and seem to be very promising for converting solar energy into electrical energy.

One of the reasons hindering the practical use of heterostructures based on CdTe and ZnTe compounds is the noticeable mismatch of their crystal lattices. As a result, mechanical stresses arise at the interfaces, which can lead to the destruction of the structure. Because of the lattice mismatch, the magnitude of the band discontinuity is known rather approximately. For example, the scatter of published data on band offset in the valence band of CdTe/ZnTe heterostructures reaches $\pm 10\%$ of the average band gap value [2].

The total band offset consists of the chemical band offset, which is determined by the chemical structure of the interface, and the deformation band offset, which is associated with the elastic energy at the interface between the contacting materials. In accordance with the „rule, the common anion/cation“ in structures with a common anion, the band offset in the valence band should be small compared to the band offset in the conduction band. Deformation can strongly change the chemical discontinuity of the bands and even lead to the formation of a type II structure. In this case, the main contribution to the potential energy of a hole is its Coulomb interaction with an electron.

In this paper, a detailed experimental study of the photoluminescence spectra and polarized reflection from structures with quantum wells with symmetric and asymmetric barriers is carried out, when the motion of holes is determined by their Coulomb interaction with an electron „trapped“ in a quantum well (QW).

2. Experiment

Structures based on $CdTe/Cd_{0.9}Zn_{0.1}Te$ with single quantum wells 8 nm wide, grown by molecular beam epitaxy in the [001] direction, were studied. A set of such structures with symmetric and asymmetric barriers was manufactured. In the first case, the quantum well was surrounded by symmetrical barriers with the composition Zn 10% on both sides, and in the second case, one of the barriers was the same as in the symmetrical structure, and the other barrier was based on $Cd_{0.4}Mg_{0.6}Te$ (Fig. 1). The height of these barriers differed by more than twice. The structure parameters are given in the caption to Fig. 1. For the buffer $Cd_{0.9}Zn_{0.1}Te$ layer in both cases, we used 1000 nm thick. The substrates had a composition of Zn 4%. Owing to the thick buffer layer, the barrier layers turned out to be

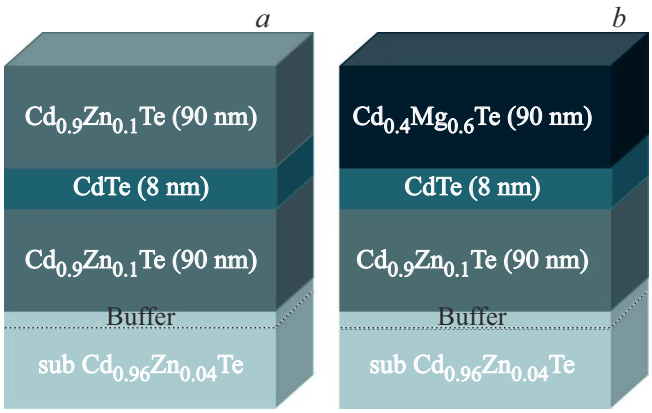

Figure 1. Scheme of the studied structures: *a* — structure with a single CdTe quantum well 8 nm wide and $Cd_{0.9}Zn_{0.1}Te$ symmetric barriers 90 nm wide. *b* — structure with a single CdTe quantum well 8 nm wide and asymmetric barriers $Cd_{0.9}Zn_{0.1}Te$ and $Cd_{0.4}Mg_{0.6}Te$ 90 nm wide each. The buffer layer with a Zn content of 10% had a thickness of the order of 1 μm.

unstressed and all mechanical stresses were applied to the quantum well.

The spectra were recorded using a monochromator with a focal length of 0.5 m and recorded with a CCD detector. A halogen lamp was used as a light source for recording transmission and reflection spectra, and a laser with a wavelength of 533 nm was used to excite photoluminescence (PL) spectra.

Figures 2, *a* and *b* show the PL spectra of structures with symmetric and asymmetric barriers, respectively. Fig. 2, *c* and *d* show the reflection spectra of these structures. The Stokes shift between the spectral features in the reflection and PL spectra was small, which indicates the high quality of these structures. It is noteworthy that both in the reflection spectra and in the PL spectra there are too many lines for the single, shallow quantum well.

Comparing the reflection and PL spectra of symmetric structures (Fig. 2, *a* and *c*), it can be seen that some resonant features are present in the reflection spectra and absent in the PL spectra. It is usually quite on the contrary, when the spectral line is present in the PL spectra and is absent or weak in the reflection spectra, which is associated with the rapid relaxation of carriers down in energy. In a structure with symmetric barriers (Fig. 2, *c*), there is a bright feature in the reflection spectrum at an energy of 1.618 eV, which is absent in the PL spectrum (Fig. 2, *a*). This can only be explained by the fact that, under nonresonant photoexcitation, carriers cannot enter this state and cannot participate in PL, but the oscillator strength of the direct optical transition to this state is rather high. In the asymmetric structure, a similar line was present in the PL spectrum. This is due to the „repulsion" of carriers from the high barrier to the well.

The most intense lines in the PL spectrum are the lines at energies of 1.596 and 1.608 eV, the intensity of other features is noticeably less. This indicates that it is difficult to relax from these states to lower energy states, and all photogenerated carriers are emitted precisely through these states.

For the initial identification of lines in the reflection spectrum, we use the result of the work [3], in which the shape of the exciton reflection contour was analyzed. In this paper, it was shown that the shape of the exciton reflection contour is determined by the interference of light reflected from the surface and from the quantum well. Depending on the phase shift during the propagation of light from the surface to the quantum well and back, the shape of the spectrum can change greatly. The reflection spectrum of the symmetric structure (Fig. 2, *a*) shows that the contour of the exciton reflection from the surface of the structure at an energy of 1.626 eV has a „differential" shape with a maximum at an energy of 1.624 eV and a minimum at an energy of 1.628 eV. The features of the reflection spectra at energies 1.597, 1.602, 1.609 and 1.620 eV have „the opposite" shape with a minimum at low energies and a maximum at higher energies.

A similar procedure was also carried out to identify the spectra of the asymmetric structure. This allows to identify the spectral features at energies 1.601, 1.604, 1.612, and 1.6.20 eV as related to the quantum well. For a more reliable identification of the observed optical transitions, we carried out theoretical calculations of the energies of exciton states.

3. Theory

Let us estimate the position of the lines of light and heavy excitons in this structure. The lattice constants in the materials $Cd_{0.9}Zn_{0.1}Te$ and CdTe differ by $\sim 0.5\%$. As a result, in addition to the potential associated with the so-called chemical band discontinuity between the contacted materials, the potential associated with the deformation band discintinuities acts on the carriers. The value of the chemical band discontinuity in the valence band of the CdTe–CdZnTe heterostructures is known very approximately and is considered to lie in the range from -10 to $+10\%$ of the total band discontinuity [4,5]. The band gaps at a temperature of 77 K for unstressed materials are $E_g^{\mathrm{CdTe}} = 1.576$ eV, $E_g^{\mathrm{Cd_{0.9}Zn_{0.1}Te}} = 1.638$ eV, $E_g^{\mathrm{Cd_{0.4}Mg_{0.6}Te}} = 2.7$ eV [6].

The value of the total chemical band offset is equal to the difference in the band gaps of bulk materials $Cd_{0.9}Zn_{0.1}Te$ and CdTe: $\Delta = E_g^{\mathrm{ZnTe}} - E_g^{\mathrm{CdTe}} = 0.065$ eV [6–8]. This value is divided between the conduction band (Δ_c) and the valence band (Δ_v), $\Delta = \Delta_c + \Delta_v$. In this paper, we assume that $\Delta_c = 0.9\Delta$ and $\Delta_v = 0.1\Delta$ [9]. Since the buffer layer and barrier layers are much thicker than the quantum well layer, it can be assumed that these layers are not stressed, and all mechanical stresses are concentrated in the well. The deformation band offset can be calculated by the formulas (1) [10,11]:

$$\Delta E_c = 2a_c(S_{11} + 2S_{12})\sigma,$$

$$\Delta E_{hh} = 2a_v(S_{11} + 2S_{12})\sigma + b(S_{11} - S_{12})\sigma,$$

$$\Delta E_{lh} = 2a_v(S_{11} + 2S_{12})\sigma - b(S_{11} - S_{12})\sigma. \qquad (1)$$

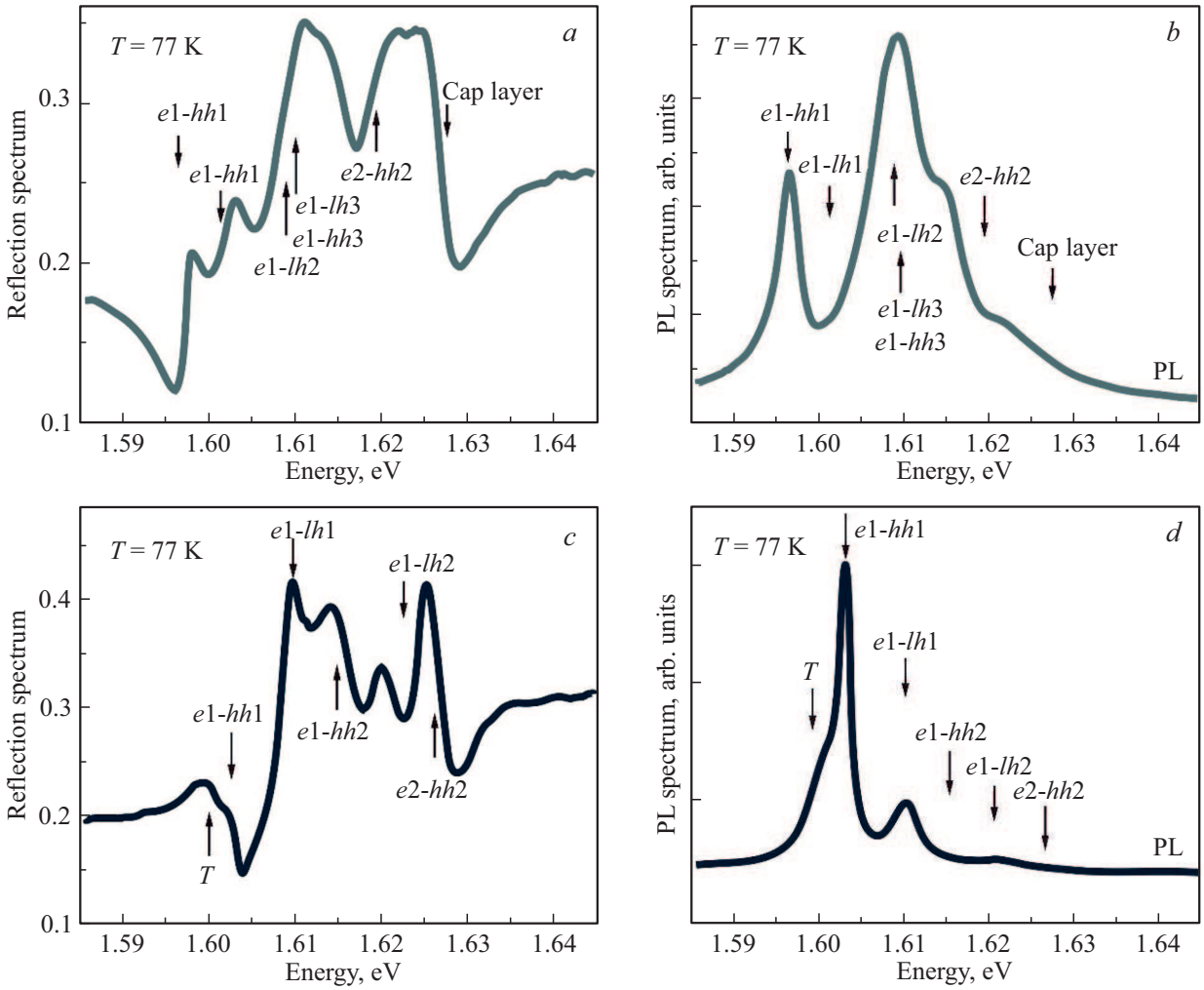

Figure 2. Reflection spectra (*a* and *c*) and photoluminescence spectra (*b* and *d*) of structures with symmetric quantum wells (*a* and *b*) and asymmetric (*c* u *d*) barriers taken at a temperature of 77 K. Arrows show optical transitions to exciton states with heavy (*hh*) and light (*lh*) holes. The identification of these transitions was carried out on the basis of calculations and is described in detail in Sec. Discussion of findings.

Here ΔE_c — deformation band offset in the conduction band, ΔE_{hh} — deformation band offset in the heavy hole band, ΔE_{lh} — deformation band offset in the light hole band, a_c and a_v — hydrostatic potentials deformations in the conduction and valence bands, b — uniaxial strain potential,$S_{ij} \cdot 10^{-11}$ m^2/H — elastic constants,

$$\sigma = \frac{\varepsilon}{(S_{11} + S_{12})}$$

— mechanical tension in the plane,

$$\varepsilon = \frac{a_j^L - a_i^L}{a_i^L}$$

— deformation in the plane. For deformation potentials, the relations [10] are valid:

$$a = a_c - a_v, \quad \frac{a_c}{a_v} = -2.$$

The values of these parameters are given in Table 1.

Table 1. Deformation potentials and elastic constants in CdTe

S_{11}	S_{12}	a, eV	b, eV	σ
3.581	−1.394	−3.85	−1.20	0.00273

Using formula (1), we obtain that the deformation band offset in the conduction band is $\Delta E_c = 11$ meV, the band offset in the heavy hole sub-band is $\Delta E_{hh} = 10.7$ meV, and the band offset in the light hole sub-band is $\Delta E_{lh} = -21.8$ meV.

The deformation band offset is summed up with the chemical band offset. Thus, due to the deformation, for light holes we obtain a heterostructure of the type II, and for heavy holes — a structure of the type 1. As a result, a total band offset in the CdZnTe/CdTe/CdZnTe structure in the conduction band is CBO = 48 meV, in the valence band of heavy holes VBO *hh* = 4.24 meV

and VBO $lh = -15.34$ meV. The band offset at the CdTe/CdMgTe interface reaches several hundred meV.

Since the magnitude of the total band offset in the valence band of the structure under study is small, their Coulomb interaction with an electron becomes the main contribution to the potential energy of holes [12].

We assume that an electron and a hole are quantized in the quantum wells for an electron and a hole formed as a result of the band discintinuity between the CdTe and CdZnTe layers and are bound to each other by the Coulomb interaction. The Schrödinger equation for an exciton in this case has the form:

$$\left[-\frac{\hbar^2}{2m_e}\frac{\partial^2}{\partial z_e^2} + V(Z_e) - \frac{\hbar^2}{2m_h}\frac{\partial^2}{\partial z_h^2} + V(z_h) - \frac{\hbar^2}{2\mu}\left(\frac{1}{\rho}\frac{\partial}{\partial\rho}\rho\frac{\partial}{\partial\rho} + \frac{1}{\rho^2}\frac{\partial^2}{\partial\phi^2}\right) - \frac{e^2}{\varepsilon\sqrt{\rho^2 + |z_e - z_h|^2}}\right] \times \Psi(\mathbf{r}_e, \mathbf{r}_h) = \left(E - \frac{\hbar^2 Q_\perp^2}{2M}\right)\Psi(\mathbf{r}_e, \mathbf{r}_h). \quad (2)$$

Here

$$\phi = \operatorname{arctg}\left(\frac{y_e - y_h}{x_e - x_h}\right), \quad \rho = \sqrt{|x_e - x_h|^2 + |y_e - y_h|^2},$$

$V(z_e)$ — rectangular potential for electrons, $V(z_h)$ — rectangular potential for holes, $\mu = \frac{m_e m_h}{m_e + m_h}$ — reduced mass, $M = m_e + m_h$ — translational exciton mass, ε — static permittivity of the QW material, Q — wave vector of the center of mass of the exciton in the plane of the QW, IE — total exciton energy counted from QW bottom.

For an approximate solution of equation (2), we use the idea of the paper [12]. Considering the motion of an electron in the quantum well „as a fast“ subsystem, we find the average potential acting on the hole from the side of the electron. To do this, we divide equation (2) into two parts:

$$\left\{\left[-\frac{\hbar^2}{2m_e}\frac{\partial^2}{\partial z_e^2} + V_e(Z_e) - \frac{\hbar^2}{2\mu}\left(\frac{1}{\rho}\frac{\partial}{\partial\rho}\rho\frac{\partial}{\partial\rho} + \frac{1}{\rho^2}\frac{\partial^2}{\partial\phi^2}\right) - \frac{e^2}{\varepsilon\rho}\right] + \left[-\frac{\hbar^2}{2m_h}\frac{\partial^2}{\partial z_h^2} + V_h(Z_h) + \frac{e^2}{\varepsilon\rho} - \frac{e^2}{\varepsilon\sqrt{\rho^2 + |z_e - z_h|^2}}\right]\right\} \times \Psi(z_e, z_h, \rho, \phi) = E\Psi(z_e, z_h, \rho, \phi). \quad (3)$$

We will consider the Hamiltonian in the first square bracket as the Hamiltonian of the „fast“ subsystem. The variables in the first square bracket are separated and the eigenfunctions of this Hamiltonian have form

$$\Phi_{n,m,l}(z_e, \rho, \phi) = \varphi_n(z_e) f_{m,l}(\rho, \phi). \quad (4)$$

In order to find them, it is necessary to solve the equation of motion of an electron in the quantum well $V(z_e)$ in the direction z and the equation of the relative motion of an electron and a hole in the plane of the well.

For an electron in a QW:

$$\left[-\frac{\hbar^2}{2m_e}\frac{\partial^2}{\partial z_e^2} + V(z_e) - E_n\right]\varphi_n(z_e) = 0. \quad (5)$$

We find the quantization energy E_n along the z axis and wave functions$\varphi_n(z_e)$ of the electron along the z. Neglecting the tails of the wave function in the barriers, we obtain:

$$E_n = \frac{\hbar^2\pi^2 n^2}{2m_e L^2},$$

$$\varphi_n(z_e) = \sqrt{\frac{2}{L}}\cos\left(n\frac{\pi}{L}z_e\right). \quad (6)$$

Here L – width of QW.

Then one need to solve the equation for a two-dimensional exciton:

$$\left[-\frac{\hbar^2}{2\mu}\left(\frac{1}{\rho}\frac{\partial}{\partial\rho}\rho\frac{\partial}{\partial\rho} + \frac{1}{\rho^2}\frac{\partial^2}{\partial\phi^2}\right) - \frac{e^2}{\varepsilon_0\rho} - E_{m,l}^{\text{ecx}}\right] f_{m,l}(\rho, \phi) = 0. \quad (7)$$

Here n — main quantum number, l — orbital quantum number. Energy spectrum of 2D exciton:

$$E_{2D}^{\text{exc}} = -\frac{\mu e^4}{2\hbar^2\varepsilon_0^2}\frac{1}{(n + |l| + 1/2)^2}.$$

Here m — main quantum number, l — orbital quantum number $l = 0, \pm1, \pm2, \ldots, \pm m$. For the ground state of the exciton ($m = 1$, $l = 0$) the wave function I2D of the exciton has the form

$$f_{1,0}(\rho, \phi) = \sqrt{\frac{2}{\pi}}\frac{2}{a_{\text{B}}}e^{-\frac{2\rho}{a_{\text{B}}}} = \sqrt{\frac{2}{\pi}}\frac{1}{\tilde{a}_{\text{B}}}e^{-\frac{\rho}{\tilde{a}_{\text{B}}}}. \quad (8)$$

Yere $\tilde{a}_{\text{B}} = \frac{a_{\text{B}}}{2}$ — Bohr radius of a two-dimensional exciton, a_{B} — Bohr radius of a bulk exciton,

$$a_{\text{B}} = \frac{\varepsilon_0\hbar^2}{\mu e^2} = \sqrt{\frac{\hbar^2}{2\mu E_{3D}^{\text{exc}}}}. \quad (9)$$

Expanding the function $\Psi(z_e, z_h, \rho, \phi)$ in equation (3) in terms of the complete system of functions $\Phi_{n,m,l}(z_e, \rho, \phi)$ and substituting into equation (3), we obtain

$$(E_n^e - E_{m,l}^{2D} - E)U_{n,m,l}(z_h) = \sum_{n',m',l'}\int dz_e d\rho d\phi \Phi_{n,m,l}^* \times \left(\frac{\hbar^2}{2m_h}\frac{\partial^2}{\partial z_h^2} - V_h(z_h) - \frac{e^2}{\varepsilon\rho} + \frac{e^2}{\varepsilon\sqrt{\rho^2 + |z_e - z_h|^2}}\right) \times U_{n',m',l'}(z_h)\Phi_{n',m',l'} = 0. \quad (10)$$

In the adiabatic approximation, leaving only the first term in this sum, we obtain

$$V_{\text{eff}}(z_h) = V(z_h) - Ry^{2D} + \frac{e^2}{\varepsilon}\frac{2}{L}\frac{2}{\pi\tilde{a}_{\text{B}}^2}\int\limits_{-L/2}^{L/2} dz_e \left|\cos\left(\frac{\pi}{L}z_e\right)\right|^2 \times \int\limits_0^{2\pi} d\phi \int\limits_0^{\infty} \rho d\rho e^{-2\rho/\tilde{a}_{\text{B}}}\left[\frac{1}{\rho} - \frac{1}{\sqrt{(\rho^2 + (z_e - z_h)^2)}}\right]. \quad (11)$$

We obtain that the effective potential acting on the hole from the side of the electron and the walls of the quantum well, has the form

$$V_{\text{eff}}(z_h) = V(z_h) + Ry^{2D} - \frac{e^2}{\varepsilon\tilde{a}_{\text{B}}}\frac{1}{L}\frac{8}{\tilde{a}_{\text{B}}}\int\limits_{-L/2}^{L/2} dz_e \left|\cos\left(\frac{\pi}{L}z_e\right)\right|^2 \times \int\limits_0^{\infty} \rho d\rho e^{-2\rho/\tilde{a}_{\text{B}}}\left[\frac{1}{\sqrt{(\rho^2 + (z_e - z_h)^2)}}\right]. \quad (12)$$

For a symmetric well, the energy levels of holes and their wave functions in this potential were found by a variational method with trial wave functions of a harmonic oscillator:

$$U_k(z_h) = \frac{1}{\sqrt{2^k k!}}\left(\frac{2}{\pi L_h}\right)^{1/4} e^{-\left(\frac{z_h}{L_h}\right)^2} H_k\left(\sqrt{\frac{2z_h}{L_h}}\right). \quad (13)$$

Trial functions used for the asymmetric well [13]:

$$U(z_h) = \left(\frac{3}{2}b^3\right)^{1/2} z_h e^{-\frac{1}{2}(bz_h)^{3/2}}. \quad (14)$$

The calculation results are given in Table 2 and 3. With these wave functions, the oscillator strengths of optical transitions were also calculated. The oscillator strengths or the radiative damping of an exciton Γ_0 in a QW are determined by the overlap integral of the electron and hole wave functions:

$$\Gamma_0 = \frac{\pi k_0 a_{\text{B}}^3}{2}\omega_{LT}\left[\int\limits_{-\infty}^{\infty} \varphi_n(z)U_k(z)dz\right]^2. \quad (15)$$

Here $\omega_{LT} \approx 0.66\,\text{meV}$ — is the longitudinal-transverse splitting of the bulk exciton in CdTe [14,15], $a_{\text{B}} = 60\,\text{A}$ — is the Bohr radius of the bulk exciton in CdTe, $k_0 = \frac{\omega}{c}$ — wave vector of light.

Figures 3, *a* and *c* show the result of calculating the potential and energy levels for light and heavy holes in a symmetric structure, while Fig. 3, *b* and *d* — in an asymmetric structure with a quantum well. The parameters were used in the calculation: $\tilde{a}_{\text{B}} \approx 30\,\text{A}$, $Ry^{2D} \approx 40\,\text{meV}$.

Electron energy at the lower size quantization level in a symmetric quantum well, counted from the bottom of the CdTe, $E_e = 20\,\text{meV}$. The energy of an electron in an asymmetric quantum well is slightly higher and equals $E_e = 23\,\text{meV}$.

4. Results and discussion

The shape of the exciton reflection contour allows one to determine the distance from the surface to the quantum well [3]. Indeed, the reflectance from a structure containing a quantum well:

$$r = r_{01} + \frac{t_{01}t_{10}e^{2i\varphi}}{1 - r_{10}r_{QW}e^{2i\varphi}}r_{QW}. \quad (16)$$

Here, the transnittance of the vacuum boundary are baoundary between vacuum and crystall — t_{10} and from the vacuum side — t_{01}; r_{01} and r_{10} — reflectances at the vacuum — crystall interface crystal from the side of vacuum and crystal, r_{QW} — reflectance from the quantum well, $\varphi = k\left(d + \frac{L}{2}\right)$ — incursion phases during the passage of light from the surface to the well, d — distance from the surface to the well, k — wave vector of light.

Neglecting multiple reflections and a contribution quadratic in r_{QW}, we obtain for the observed reflectance:

$$R = |r|^2 \approx R_0\left[1 + 2\frac{t_{01}t_{10}}{r_{01}}\text{Re}\{r_{QW}e^{2i\varphi}\}\right]. \quad (17)$$

Thus, the shape of the reflection spectrum is determined by the phase shift φ of light waves reflected from the surface and reflected from the quantum well. The thickness of the outer barrier in our structures is 90 nm, the refractive index of light in CdZnTe in this spectral area is $n = 3.3$. From this we obtain that the phase shift of the light wave during the passage of the barrier layer is approximately equal to π. Thus, the shape of the contour of the exciton reflection from the well should be inverse to the shape of the contour of the reflection from the surface, which is seen in the spectra (Fig. 2, *c*). Thus, the features of the reflection spectra at energies 1.597, 1.602, 1.609, and 1.620 eV should be attributed to exciton transitions in the quantum well.

The only difference between the asymmetric structure and the symmetric one is that in the CdMgTe barrier layer, the refraction index for the energies of exciton resonances in the quantum well is equal to $n = 2.45$. In this case the phase shift of the light wave passing of the barrier layer is approximately equal to $\pi/2$. This allows to identify the spectral features at energies 1.601, 1.604, 1.612, and 1.6.20 eV as related to the quantum well. These values are slightly higher than the energies of exciton transitions in a symmetric quantum well. Indeed, for a well with asymmetric barriers, the energy level should be slightly higher than for a well with symmetric barriers. In an asymmetric structure, the shape of the contour of the exciton reflection from the CdZnTe barrier is the same as from the well. Since this barrier is located at the same distance from the surface, the phase shift of the light wave reflected from the well and from the CdZnTe layer during the passage of the layer from the well to the surface is practically the same.

Using formulas (16), (17), the exciton reflection spectra from a symmetric and asymmetric structure with a quantum

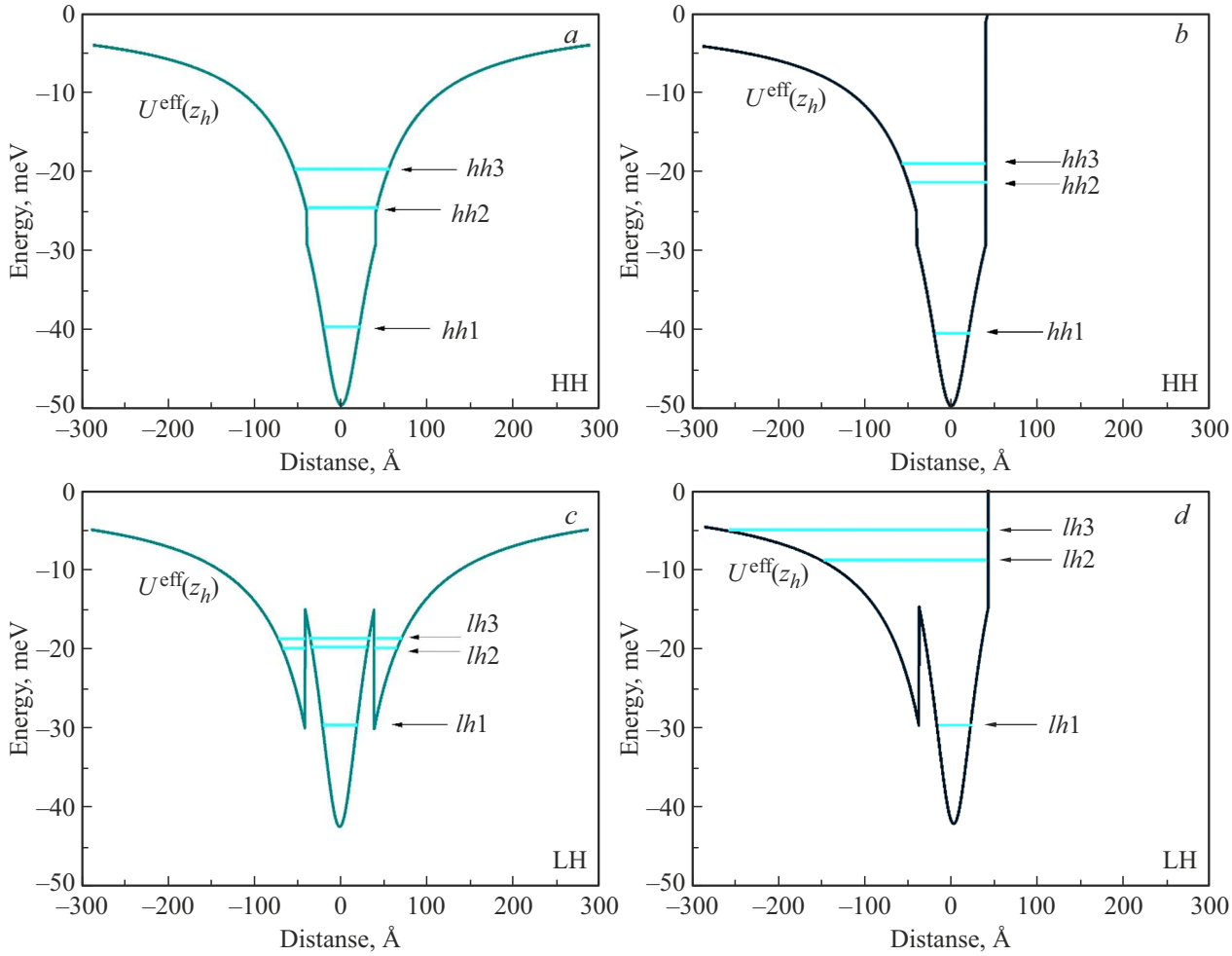

Figure 3. Calculation of the effective potential created by an electron and the energy levels of holes in a quantum well. $U^{\text{eff}}(z_h) = U(z_h) + U^{(\text{coulomb})}(z_h)$ — effective potential acting on a hole, counted from the top of the valence band of the CdZnTe barrier. (a, b) — heavy holes in symmetric and asymmetric wells, (c u d) — light holes in symmetric and asymmetric pits, respectively.

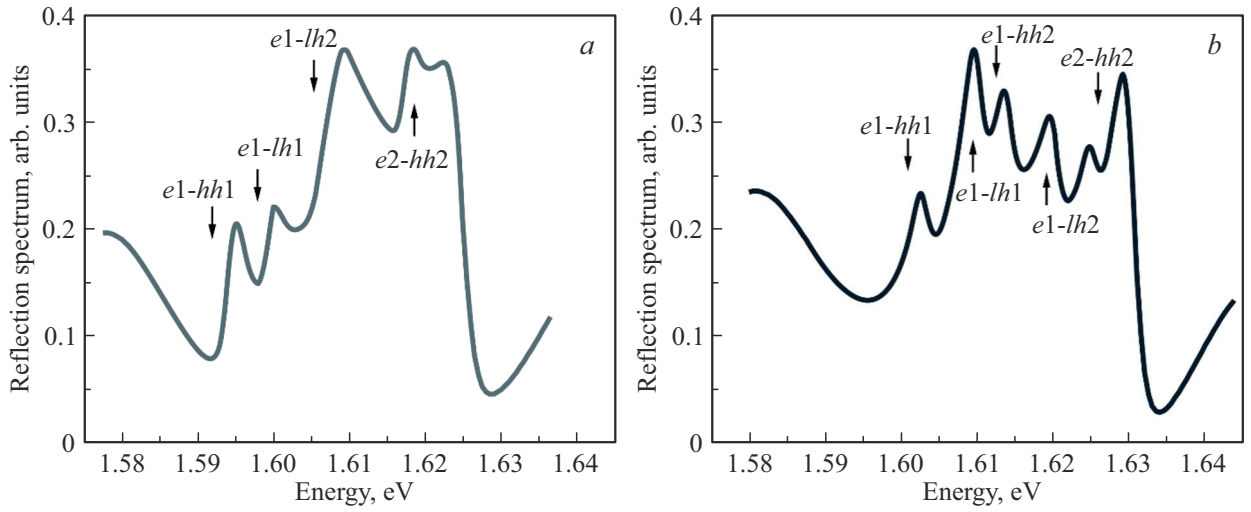

Figure 4. Exciton reflection spectra from symmetric (a) and asymmetric (b) structures with a quantum well, calculated using formulas (12)–(15).

Table 2. Symmetric well

Experiment, eV	Calculation, eV	Transition	Experiment Γ_0, meV	Calculation of Γ_0, rel.un.	Experiment Γ, meV
1.597	1.598	$e1-hh1$	0.9	0.5	1.5
1.602	1.605	$e1-lh1$	0.6	0.2	1.5
	1.612	$e1-lh2$	0.23	0.1	1.4
1.609	1.613	$e1-lh3$	0.23	0.1	1.4
	1.613	$e1-hh3$	0.23	0.1	1.4
1.6185	1.620	$e2-hh2$	0.048	0.2	1.9
1.6265	1.6265	Barrier	$\omega_{LT} = 0.65$	–	2.3

Table 3. Asymmetric well

Experiment, eV	Calculation, eV	Transition	Experiment Γ_0, meV	Calculation of Γ_0, rel.un.	Experiment Γ, meV
1.600	–	Trion	–	–	–
1.604	1.603	$e1-hh1$	0.8	1.0	1.3
1.611	1.612	$e1-lh1$	0.4	0.4	1.5
1.614	1.619	$e1-hh2$	0.2	0.4	1.0
1.621	1.625	$e1-lh2$	0.2	0.4	1.3
1.625	1.627	$e2-hh2$	0.2	0.3	1.4
1.631	1.630	Barrier	–	–	–

well (Fig. 4, *a* and *b*) were calculated for comparison with the spectra obtained in the experiment (Fig. 2, *a* u *c*).

The radiative and non-radiative exciton damping can be estimated from the experimental spectra. Amplitude factor of exciton reflection from a single quantum well [16]:

$$r_{QW} = \frac{i\Gamma_0}{\omega_0 - \omega - i(\Gamma_0 + \Gamma)}. \qquad (18)$$

Here Γ_0 — radiative exciton damping, Γ — non-radiative damping, ω_0 — exciton resonance frequency.

Thus, the width of the exciton reflection contour is 2Γ, and the amplitude of the reflection contour is Γ_0/Γ. Comparison of the results obtained by numerical calculation, reflection spectra and PL spectra is given in Tables 2 and 3. First of all, the question arises — why some exciton states appear in the reflection spectra in the form of bright lines, but are completely absent in the PL spectra. It usually happens the other way around: due to energy relaxation, carriers accumulate in lower energy states, from which PL occurs. As a result, the PL intensity can be significant even at a low optical transition oscillator strength.

Under nonresonant photoexcitation, holes rapidly lose energy, relaxing to the bottom of the corresponding bands. In our structure for heavy holes (hh) this is a quantum well (QW) with a depth of 4.2 meV, and for light holes (lh) these are CdTe layers with a height of 15.3 meV (Fig. 3). Light holes quickly pass from these layers to CdZnTe layers, where their energy is lower.

Electrons arrive at the bottom of their band much later than holes. This is confirmed by their greater mobility compared to holes and, consequently, a lower rate of energy loss. Once at the lower size quantization level in the QW, they begin to bind with holes, forming excitons. First, highly excited bound states with a large radius are formed. Electrons and holes, emitting first acoustic phonons and then optical ones, „descend“ in energy to the ground state of the exciton [17].

Those light holes, which at the time of electron arrival in the QW, ended up in the CdZnTe layers, form excitons ($e1-lh2$). However, there are no holes in the CdTe layers at the moment when the electrons arrive, and such excitons ($e1-lh1$) are not formed.

Thus, holes that entered the CdTe layers before the arrival of electrons cannot form excitons, and such excitons are not observed in the PL spectra. However, these excitons ($e1-lh1$) are clearly manifested in the reflection spectra, since their formation does not require an intermediate process of binding and energy relaxation.

In asymmetric structures, such a transition is seen both in the reflection spectrum and in the photoluminescence spectrum. This is due to the fact that the high CdMgTe barrier effectively repels holes and prevents them from escaping from the quantum well.

The calculation shows that due to the fact that the potential for holes strongly „expands“ with increasing energy, the quantization levels of holes approach each other. Thus, the distance between hole levels in a symmetric QW: $hh2$, $hh3$; $lh2$ and $lh3$ does not exceed 2 meV. Thus, all these levels practically overlap and appear in the spectra at the same energy as a single line (the $e1-lh2$ line in Fig. 2, *c*).

Indeed, in the PL and reflection spectra of the symmetrical structure in Fig. 2, *a* u *c*, it can be seen that the $e1-lh2$

transition, which should be symmetry-forbidden, appears as a bright line. This is explained by the fact that the levels of light and heavy holes are *hh*2, *hh*3; *lh*2 and *lh*3 are very close to each other in terms of energy. As a result, even a slight perturbation, for example, due to a weak asymmetry of the structure, leads to their mixing, and this transition manifests itself in the spectra.

5. Conclusion

The polarized reflection spectra from strained quantum well structures with symmetric $Cd_{0.9}Zn_{0.1}Te/CdTe/Cd_{0.9}Zn_{0.1}Te$ and asymmetric $Cd_{0.9}Zn_{0.1}Te/CdTe/Cd_{0.4}Mg_{0.6}Te$ barriers have been studied. A feature of these structures is that the band offset in the valence band is very small. As a result, due to the deformations caused by the mismatch between the lattice constants of the materials of the wells and barriers, the band diagram for heavy holes was of type I, and for light holes — type II. Meanwhile, the binding energy of the exciton was several times greater than the band offset in the valence band. This led to the fact that a rather „unusual" potential acted on the hole from the side of the electron and the potential of the quantum well. This potential, the levels of carrier quantization in the structure, and the radiative damping of the ground and excited states of the exciton are calculated. The calculation showed good agreement with the values obtained from the analysis of the reflection spectra without the use of fitting parameters.

In structures with symmetric barriers, exciton resonances were found in the reflection spectra, which do not appear in the photoluminescence spectra. This feature is explained by the impossibility of populating some states upon non-resonant optical excitation.

Acknowledgments

The authors are grateful to L.E. Golub and E.L. Ivchenko for useful discussions.

Funding

The paper was carried out with the financial support of the project from the Russian Science Foundation, No. 21-12-00304.

Conflict of interest

The authors declare that they have no conflict of interest.

References

[1] *Comprehensive Guide on Organic and Inorganic Solar Cells. Fundamental Concepts to Fabrication Methods.* A volume in Solar Cell Engineering, ed. by Md. Akhtaruzzaman and Vidhya Selvanathan (Academic Press, 2022).
[2] D.J. Dunstan, A.D. Prins, B. Gil, J.P. Faurie. Phys. Rev. B, **44** (8), 4017 (1991).
[3] E.L. Ivchenko, P.S. Kopiev, V.P. Kochereshko, I.N. Uraltsev, D.R. Yakovlev, S.V. Ivanov, B.Ya. Meltser, M.A. Kalitievsky. Semiconductors, **22** (5), 784 (1988). (in Russian).
[4] H. Mathieu, J. Allegre, A. Chatt, P. Lefebre, J.P. Faurie. Phys. Rev. B, **38** (11), 7740 (1988).
[5] H. Tuffigo, N. Magnea, H. Mariette, A. Wasiela, Y. Merle d'Aubigne. Phys.Rev. B, **43** (18), 14629 (1991).
[6] Landolt-Bornstein. *Numerical Data and Functional Relationship in Science and Technology,* ed. by W. Martienssen. Group III: Condens. Matter (Springer, 2000).
[7] E. Deleporte, J.M. Berroir, G. Bastard, C. Delalande, J.M. Hong, L.L. Chang. Phys. Rev. B, **42** (9), R5891 (1990).
[8] E. Deleporte J.M. Berroir, C. Delalande, N. Magnea, H. Mariette, J. Allegre, J. Calatayud. Phys. Rev. B, **45** (11), R6305 (1992).
[9] N.G. Filosofov, A.Y. Serov; G. Karczewski, V.F. Agekian, H. Mariette, V.P. Kochereshko. AIP Advances, **10** (8), 085224 (2020).
[10] H. Mariette, F. Dal'bo, N. Magnea, G. Lentz, H. Tuffigo. Phys. Rev. B, **38** (17), 12443 (1988).
[11] P. Peyla, Y. Merle d'Aubigne, A. Wasiella, R. Romestain, H. Mariette, M.D. Sturge, N. Magnea, H. Tuffigo. Phys. Rev. B, **46** (3), 1557 (1992).
[12] Al.L. Efros. Fiz. Tekh. Poluprovodn., **20** (7), 1281 (1986). (in Russian).
[13] Y. Takada, Y. Uemura. J. Phys. Soc. Jpn., **43**, 139 (1977).
[14] E.L. Ivchenko, A.V. Kavokin, V.P. Kochereshko, G.R. Pozina, I.N. Uraltsev, D.R. Yakovlev, R.N. Bicknell-Tassius, A. Waag, G. Landwehr. PRB, **46**, 7713 (1992).
[15] H. Tuffigo, R.T. Cox, N. Magnea, Y. Merle d'Aubigne, A. Million. PRB, **37**, 4310 (1988).
[16] E.L. Ivchenko. *Optical Spectroscopy of Semiconductor Nanostructures* (Alpha Science Int., Harrow, UK, 2005).
[17] V.N. Abakumov, L.N. Kreschuk, I.N. Yassievich. Semiconductors, **12**, 152 (1977). (in Russian).

Translated by E.Potapova